

# Properties of Convex Optimal Power Flow Model for Meshed Power Networks

Zhao Yuan, *Member, IEEE*, Mario Paolone, *Senior Member, IEEE*

**Abstract**—In this paper, we firstly discuss the compression of the approximation gap of the convex optimal power flow (OPF) model based on the branch flow formulation by deriving branch ampacity constraint associated to its power losses. Then, we rigorously prove that: (i) the approximated voltage phase angle constraint, required to make the branch flow model valid for both radial and meshed power networks, is a relaxation of the original nonconvex AC optimal power flow (o-ACOPF) model; (ii) it is possible to infer necessary conditions to recover a feasible solution of the o-ACOPF model from the optimal solution of the convex second-order cone ACOPF (SOC-ACOPF) model; (iii) it is possible to derive the expression of the global optimal solution of the o-ACOPF model providing that the relaxation of the SOC-ACOPF model is tight; (iv) the (parametric) optimal value function of the ACOPF or SOC-ACOPF model is monotonic with regarding to load absorptions if the objective function is monotonic with regarding to the nodal power injections; (v) tight solutions of the SOC-ACOPF model always exist when load absorptions become large enough. Numerical simulations for IEEE power network test cases to validate our analytical proofs are given and discussed.

**Index Terms**—Optimal Power flow, ampacity constraint, tight solution, second-order cone programming.

## NOMENCLATURE

### Sets:

- $\mathcal{N}$  Nodes (or buses).
- $\mathcal{L}$  Lines (or branches).

### Variables:

- $p_n, q_n$  Active and reactive power injections at node  $n$ .
- $p_{sl}, q_{sl}$  Non-measurable sending- end active and reactive power flows for branch  $l$ .
- $p'_{sl}, q'_{sl}$  Measurable sending- end active and reactive power flows for branch  $l$ .
- $p_{rl}, q_{rl}$  Non-measurable receiving- end active and reactive power injection of branch  $l$ .
- $p'_{rl}, q'_{rl}$  Measurable receiving- end active and reactive power injection of branch  $l$ .
- $q_{csl}, q_{crl}$  Sending- and receiving- end shunt reactive power of branch  $l$ .
- $i_{sl}, i_{rl}$  Non-measurable sending- and receiving- end current flows of branch  $l$ .
- $i'_{sl}, i'_{rl}$  Measurable sending- and receiving-end current flows of branch  $l$ .
- $p_{ol}, q_{ol}$  Active and reactive power losses of branch  $l$ .
- $v_n, V_n$  Phase-to-ground voltage magnitude and voltage square at node  $n$ .
- $v_{sl}, v_{rl}$  Sending- and receiving- end phase-to-ground voltage of branch  $l$ .

- $V_{sl}, V_{rl}$  Sending- and receiving- end phase-to-ground voltage square of branch  $l$ .
- $\theta_n$  Phase-to-ground voltage phase angle at node  $n$ .
- $\theta_l$  Phase angle difference between sending- and receiving- end phase-to-ground voltages of branch  $l$ .
- $\theta_{sl}, \theta_{rl}$  Phase angles of sending- and receiving- end phase-to-ground voltages of branch  $l$ .
- $K_{o_l}$  Equivalent ampacity constraint for power losses of branch  $l$ .

### Parameters:

- $A_{nl}^+, A_{nl}^-$  Node to line (branch) incidence matrix.
- $X_l, R_l$  Longitudinal reactance and resistance of branch  $l$  modelled as a passive  $\pi$  equivalent.
- $G_n, B_n$  Shunt conductance and susceptance of node  $n$ .
- $B_{sl}, B_{rl}$  Sending- and receiving-end shunt susceptance of branch  $l$ .
- $K'_l, K_l$  Actual and approximated ampacity of branch  $l$ .
- $p_n^{min}, p_n^{max}$  Lower and upper bound of  $p_n$ .
- $q_n^{min}, q_n^{max}$  Lower and upper bound of  $q_n$ .
- $\theta_l^{min}, \theta_l^{max}$  Lower and upper bound of  $\theta_l$ .
- $p_{dn}, q_{dn}$  Active and reactive load absorptions of node  $n$ .
- $\alpha_n, \beta_n$  Cost parameters of nodal active power injection.

## I. INTRODUCTION

OPTIMAL power flow (OPF) is a fundamental mathematical optimization model for decision making in power system operation and planning [1]. Improving the solution quality of OPF can give large economic and engineering benefits to the power industry [2], [3]. Recent literature focusing on the convexification of the OPF model suffered from inexactness due to the relaxation of several constraints [4]–[14].

The branch flow formulation of the power flow equations for radial power networks has been originally derived by Baran and Wu in [15] to optimize the placement of capacitor in radial distribution networks. In [16], Jabr derives a conic programming approach to solve load flow in radial distribution network. In [4], Farivar and Low propose the branch flow model as a relaxed OPF model by relying on second-order cone programming (SOCP) and prove that the relaxation is tight for radial networks under the assumption that the upper bound of power generation is infinite. In [5], Gan, Li et al. prove that the optimal solution of the branch flow model is exact (tight) if the voltage upper bounds are not binding and the network parameters satisfy some mild conditions which can be checked *a priori*. Christakou, Tomozei et al. show in [17] that the branch flow model is not exact due to the approximation of the ampacity constraint of the branch. Nick et al. propose an exact convex OPF model for radial distribution networks

in [18] by considering the shunt parameters associated to the exact modelling of the lines or other branch elements. Sufficient conditions regarding the network parameters under which the convex OPF model in [18] can give exact solutions to the original ACOPF are provided and rigorously proved. In [6], Kocuk, Dey et al. propose three methods (arctangent envelopes, dynamic linear inequalities and separation over cycle constraints) to strengthen i.e. tighten SOCP relaxation of OPF. Numerical results show better solution quality of SOCP-based model over SDP-based model [6].

Semidefinite programming (SDP) relaxation of OPF has been firstly proposed by Bai et al. in [7]. The proposed procedures derive the rectangular form OPF in a quadratic programming model and replace the variable-vector ( $\mathbf{x}$ ) by the variable-matrix ( $X = \mathbf{x}^T \mathbf{x}$ ). Solutions of OPF can be recovered from the square roots of the diagonal elements in the variable-matrix [7]. SDP advantages in avoiding the derivation of Jacobian and Hessian matrices if the interior point method (IPM) is used [7]. However, severe computational burden exists for large-scale power networks [7]. Lavaei and Low propose to solve the SDP relaxation of the dual OPF problem [8]. They prove that sufficient and necessary condition of zero duality gap holds for several IEEE test cases (14, 30, 57, 118) at the the base power load levels.<sup>1</sup> But the branch ampacity constraint is not fully addressed.

Based on polynomial optimization theory, Molzahn and Hiskens propose the moment-based relaxations of OPF in [9]. This formulation firstly defines order- $\gamma$  moment relaxation  $x_\gamma$  of all monomials  $\hat{x}^\alpha$  of voltage real-and-imaginary components  $\hat{x}$ . Then, all the monomials  $\hat{x}^\alpha$  up to order  $2\gamma$  constitute the symmetric moment matrix  $M_\gamma$  which is used to re-formulate the OPF constraints via the SDP. Global optimal solutions are found, at the cost of heavy computational burden due to higher relaxation order  $\gamma$ , for the test cases in [9]. The same authors in [10] improve the computational efficiency of this method by exploiting power system sparsity and applying high relaxation order to specific buses.

In [11], Hijazi, Coffrin et al. propose a quadratic convex (QC) relaxation by replacing the nonconvex voltage-amplitudes-and-phase-angle associated constraints with the corresponding convex envelopes. In [12], the same authors investigate the relationships between different convex OPF formulations including QC, SDP and SOCP. Theoretical results show that, for the models considered in [12], the QC relaxation is stronger than other formulations. Reducing the optimality gap of QC or SOCP based OPF models by bound tightening techniques can be found in [13], [14].

Recently, Shchetinin et al. propose in [19] three methods which require solving optimization problems to tighten the upper bounds of the voltage phase angle difference in order to satisfy the branch ampacity constraint. The same authors in [20] propose an iterative algorithm to construct a number of linear constraints (based on inner or outer approximation) to approximate the branch ampacity constraint. In this paper,

we focus on the formal derivation of equivalent ampacity constraint for the branch power losses.

More specifically, we consider to improve the convex OPF in meshed power networks which necessitates the additional voltage phase angle constraint. Instead of using the approach in [18] to reformulate the branch flow model, we keep using the same set of variables (in the form of power flow variables) of the branch flow model but equivalently derive the ampacity constraint for the power losses. In this way, we overcome the approximation gap due to neglecting of the shunt elements of the branches. We then propose six theorems supporting the proposed SOC-ACOPF model. In this regard, the main contributions of this paper are: (i) derivation of the branch ampacity constraint for the power losses; (ii) proving that the SOC-ACOPF model (with additional constraint to improve its feasibility towards the original ACOPF constraints) is a relaxed ACOPF model; (iii) deriving a feasible solution recovery procedure when the SOC relaxation is tight; (iv) demonstrating that the (parametric) optimal value functions of the SOC-ACOPF model and o-ACOPF model are monotonic with regarding to nodal load absorptions when the objective function is monotonic with regarding to nodal power injections; (v) explaining that larger load absorptions can tighten the relaxation in the SOC-ACOPF model.

The rest of this paper is organized as follows. Section II formulates the o-ACOPF model and SOC-ACOPF model for meshed power networks. Section III derives the equivalent ampacity constraint of the branch for the power losses. Section IV proposes and proves important properties of the SOC-ACOPF model. Section V gives the numerical validations of our analytical proofs and discussions. Section VI concludes.

## II. OPTIMAL POWER FLOW MODEL

### A. Power based Branch Flow Model

We assume that the three-phase power grid satisfies two conditions: (i) all the branches and shunt impedances are circularly symmetric; (ii) all the triplets of nodal voltages and branch currents are symmetrical and balanced. These two conditions validate the use of single-line equivalent model of the three-phase power grid. The full ACOPF model is based on the validated branch flow model illustrated in [21]. We denote this original ACOPF model as o-ACOPF (1). The variable convention makes reference to the branch  $\pi$  model in Fig. 1.

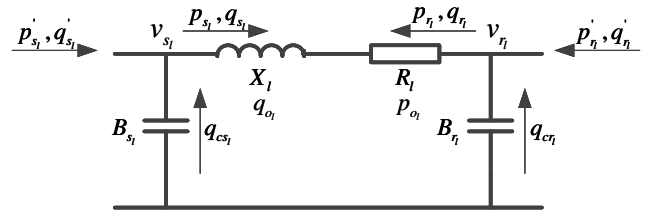


Fig. 1. The branch II model and associated variables

The subscripts  $s, r, d, o$  in  $p_{\cdot}, q_{\cdot}, v_{\cdot}, V_{\cdot}, p_{\cdot}, q_{\cdot}$  are not indices but only implies the meaning of sending-end of branch

<sup>1</sup> As a comparison, in this paper, we evaluate the OPF solutions of IEEE test cases at low power load levels (for which the relaxation gaps are prominent).

$l$ , receiving-end of branch  $l$ , load absorptions and power losses, correspondingly. Note  $(p'_{s(r)_l}, q'_{s(r)_l})$  are the actual (i.e. measurable) branch power flows. The variables  $(p_{s(r)_l}, q_{s(r)_l})$  are the non-measurable branch power flows used in our OPF model. For the differences between  $(p'_{s(r)_l}, q'_{s(r)_l})$  and  $(p_{s(r)_l}, q_{s(r)_l})$ , or between  $i'_{s(r)_l}$  and  $i_{s(r)_l}$ , please refer to references [17] and [18]. More details about the relationship between  $(p'_{s(r)_l}, q'_{s(r)_l})$  and  $(p_{s(r)_l}, q_{s(r)_l})$  are derived later in this paper.

$$\text{Minimize}_{\Omega} \quad f(p_n, q_n, p_{o_l}, q_{o_l}) \quad (1a)$$

subject to

$$p_n - p_{d_n} = \sum_l (A_{nl}^+ p_{s_l} - A_{nl}^- p_{o_l}) + G_n V_n, \quad \forall n \in \mathcal{N} \quad (1b)$$

$$q_n - q_{d_n} = \sum_l (A_{nl}^+ q_{s_l} - A_{nl}^- q_{o_l}) - B_n V_n, \quad \forall n \in \mathcal{N} \quad (1c)$$

$$p_{o_l} = \frac{p_{s_l}^2 + q_{s_l}^2}{V_{s_l}} R_l, \quad \forall l \in \mathcal{L} \quad (1d)$$

$$q_{o_l} = \frac{p_{s_l}^2 + q_{s_l}^2}{V_{s_l}} X_l, \quad \forall l \in \mathcal{L} \quad (1e)$$

$$V_{s_l} - V_{r_l} = 2R_l p_{s_l} + 2X_l q_{s_l} - R_l p_{o_l} - X_l q_{o_l}, \quad \forall l \in \mathcal{L} \quad (1f)$$

$$v_{s_l} v_{r_l} \sin \theta_l = X_l p_{s_l} - R_l q_{s_l}, \quad \forall l \in \mathcal{L} \quad (1g)$$

$$\begin{aligned} i'_{s(r)_l} &= \frac{p_{s(r)_l}^2 + q_{s(r)_l}^2}{V_{s(r)_l}} \\ &= \frac{p_{s(r)_l}^2 + (q_{s(r)_l} + q_{cs(r)_l})^2}{V_{s(r)_l}} \leq K'_l, \quad \forall l \in \mathcal{L} \end{aligned} \quad (1h)$$

$$V_n = v_n^2, \quad \forall n \in \mathcal{N} \quad (1i)$$

$$v_n^{\min} \leq v_n \leq v_n^{\max}, \quad \forall n \in \mathcal{N} \quad (1j)$$

$$\theta_l^{\min} \leq \theta_l \leq \theta_l^{\max}, \quad \forall l \in \mathcal{L} \quad (1k)$$

$$p_n^{\min} \leq p_n \leq p_n^{\max}, \quad \forall n \in \mathcal{N} \quad (1l)$$

$$q_n^{\min} \leq q_n \leq q_n^{\max}, \quad \forall n \in \mathcal{N} \quad (1m)$$

Where  $\Omega = \{p_n, q_n, p_{s_l}, q_{s_l}, p_{o_l}, q_{o_l}, V_n, v_n, \theta_l\} \in \mathbb{R}^m$  is the set of model variables.<sup>2</sup> Based on the applications, the objective function  $f(p_n, q_n, p_{o_l}, q_{o_l})$  can be the economic cost of energy production, network power losses or security margin. In this paper, we assume the objective function to be convex. Equations (1b) and (1c) represent the active and reactive power balance.  $A_{nl}^+$  and  $A_{nl}^-$  are the incidence matrices of the network with  $A_{nl}^+ = 1$ ,  $A_{nl}^- = 0$  if  $n$  is the sending-end of branch  $l$ , and  $A_{nl}^+ = -1$ ,  $A_{nl}^- = -1$  if  $n$  is the receiving-end of branch  $l$ .  $V_{s_l} = v_{s_l}^2$  and  $V_{r_l} = v_{r_l}^2$  are voltage magnitude squares. Equations (1d)-(1e) represent active power and reactive power losses.  $\theta_l = \theta_{s_l} - \theta_{r_l}$  is the voltage phase angle difference of branch  $l$ . Constraints (1b)-(1g) make the o-ACOPF model valid for both radial and meshed power networks. Equations (1f)-(1g) are derived by taking the magnitude and phase angle of the voltage drop phasor along branch  $l$  respectively. To guarantee this derivation is valid, we need that  $(\theta_l^{\min}, \theta_l^{\max}) \subseteq (-\frac{\pi}{2}, \frac{\pi}{2})$ . Constraints (1j)-(1m) are bounds for voltage magnitude, voltage phase angle difference, nodal active power injection and nodal reactive power injection. This

model is nonconvex because of the constraints (1d), (1e), (1g) and (1i). Current available nonlinear programming solvers are unable to efficiently find the global optimal solution of this nonconvex model.

### B. Second-Order Cone Relaxation

The SOC-ACOPF model is derived using branch sending-end power injections and voltage phase angle difference variables. Note that in the derived model, voltage square variables are included (voltage can be recovered from the model by taking the square root of the voltage square solutions). SOC-ACOPF is set out in (2).

$$\text{Minimize}_{\Omega} \quad f(p_n, q_n, p_{o_l}, q_{o_l}) \quad (2a)$$

subject to

$$(1b) - (1c), (1f), (1j) - (1m)$$

$$K_{o_l} \geq q_{o_l} \geq \frac{p_{s(r)_l}^2 + q_{s(r)_l}^2}{V_{s(r)_l}} X_l, \quad \forall l \in \mathcal{L} \quad (2b)$$

$$p_{o_l} X_l = q_{o_l} R_l, \quad \forall l \in \mathcal{L} \quad (2c)$$

$$\theta_l = X_l p_{s_l} - R_l q_{s_l}, \quad \forall l \in \mathcal{L} \quad (2d)$$

Constraints (2b)-(2c) represent active power and reactive power losses. The left side of (2b) bounds  $q_{o_l}$ , which equivalently bounds the ampacity of branch  $l$  as explained in the next section. Using this constraint, it is possible to introduce larger power losses values than the actual ones in constraints (1b)-(1c) and (1f). Equation (2d) is approximated from the nonconvex constraint (1g). This approximation is based on the assumption  $v_{s_l} v_{r_l} \sin \theta_l \approx \theta_l$ . The left side of equation (2d) can also be derived by the first-order Taylor series expansion of  $v_{s_l} v_{r_l} \sin \theta_l$  for  $v_{s_l} = v_{r_l} = 1$  and  $\theta_l = 0$ . We will show later that using (2d) actually relaxes the ACOPF model when  $v_n \in (0.9, 1.1)$  and  $\theta_l \in (-\frac{\pi}{2}, \frac{\pi}{2})$ . Using constraint (2d) (to replace constraint (4a)) doesn't affect other constraints in the model.

### III. DERIVING THE AMPACITY CONSTRAINT FOR THE POWER LOSSES

Since the actual measurable power flows  $(p'_{s_l}, q'_{s_l})$  and current  $i'_{s(r)_l}$  are different from the power flow variables  $(p_{s_l}, q_{s_l})$  and  $i_{s(r)_l}$  that we are using in the SOC-ACOPF model, it is necessary to derive the gap between  $i'_{s(r)_l}$  and  $i_{s(r)_l}$  to quantify  $K_l, K_{o_l}$  according to the known parameter  $K'_l$ . From Fig. 1, we have:

$$p'_{s(r)_l} = p_{s(r)_l} \quad (3a)$$

$$q'_{s(r)_l} = q_{s(r)_l} - q_{cs(r)_l} \quad (3b)$$

$$q_{cs(r)_l} = V_{s(r)_l} B_{s(r)_l} \quad (3c)$$

Where  $q_{cs(r)_l}$  is the reactive power injection from the sending-(receiving-) end shunt capacitance for the branch  $l$ ,  $B_{s(r)_l}$  is the shunt susceptance. The ampacity of branch  $l$  is constrained as:

$$\|i'_{s(r)_l}\|^2 = \frac{p_{s(r)_l}^2 + q_{s(r)_l}^2}{V_{s(r)_l}} \leq K'_l \quad (3d)$$

<sup>2</sup>Note this is not the set of state variables. The state variables are  $\{v_n, \theta_l\}$ .

From (3a)-(3d), we can derive the gap  $\Delta^2 I$  between  $\|i_{s(r)l}\|^2$  and  $\|i'_{s(r)l}\|^2$ :

$$\begin{aligned}\Delta^2 I &= \|i_{s(r)l}\|^2 - \|i'_{s(r)l}\|^2 \\ &= \frac{-q_{cs(r)l}^2 + 2q_{s(r)l}q_{cs(r)l}}{V_{s(r)l}} \\ &= \frac{-V_{s(r)l}^2 B_{s(r)l}^2 + 2q_{s(r)l}V_{s(r)l}B_{s(r)l}}{V_{s(r)l}} \\ &= -V_{s(r)l}B_{s(r)l}^2 + 2q_{s(r)l}B_{s(r)l}\end{aligned}\quad (3e)$$

The branch ampacity constraint (3d) is equivalent to:

$$i_{s(r)l}^2 = \frac{p_{s(r)l}^2 + q_{s(r)l}^2}{V_{s(r)l}} \leq K_l' + \Delta^2 I \quad (3f)$$

Or:

$$K_l = K_l' + \Delta^2 I \quad (3g)$$

The reactive power losses upper bounds  $K_{ol}$  can be quantified as:

$$\begin{aligned}K_{ol} &= K_l X_l \\ &= (K_l' + \Delta^2 I) X_l \\ &= (K_l' - V_{s(r)l}B_{s(r)l}^2 + 2q_{s(r)l}B_{s(r)l}) X_l\end{aligned}\quad (3h)$$

Note equation (3h) is linear. So, if we use the expression of  $K_{ol}$  from (3h) in the constraint (2b), the SOC-ACOPF model (2) is still convex and we avoid any approximation on the branch ampacity constraint.

It is worth to mention that using  $K_{ol}$  to constrain the upper bound of power losses  $p_{ol}$  in (2b) is more realistic than constraining the power flows  $(p'_{sl}, q'_{sl})$  or  $(p_{sl}, q_{sl})$  in the way of  $p_{sl}^{(')2} + q_{sl}^{(')2} \leq S_l$  (where  $S_l$  is the maximum branch power flow). This is because:

- the branch ampacity is given by the manufacturers in the form of maximum current  $i'_{s(r)l} = \sqrt{K_l'}$ .
- the temperature increase of the branch (which lead to insulation degrading) is actually caused by the power losses due to the current which is the typical variable constrained by the branch manufacturer.
- the voltage amplitudes  $v_{s(r)l}$  of both ends of the branch are varying during the grid operations. The maximum allowed power capacity  $S_l$  of the branch would then depend on the nodal voltage amplitudes at the branch ends.

#### IV. PROPERTIES OF THE SOC-ACOPF MODEL

##### Theorem 1

Assume  $v_n \in (0.9, 1.1)$  and  $\theta_l \in (-\frac{\pi}{2}, \frac{\pi}{2})$ , replacing (1g) by (2d) relaxes the o-ACOPF model (1) i.e. the SOC-ACOPF model (2) is a relaxation of the o-ACOPF model (1) (rather than an approximation of the o-ACOPF model).

*Proof.* We prove this theorem by showing that any point in the feasible region of o-ACOPF model (1) can always map to a point located in the feasible region of the SOC-ACOPF model (2). However, the reverse statement does not hold. In other

words, some feasible solutions of the SOC-ACOPF model (2) are not feasible for the o-ACOPF model (1). Suppose  $\Omega_0 = \{p_{0,n}, q_{0,n}, p_{0,sl}, q_{0,sl}, p_{0,ol}, q_{0,ol}, V_{0,n}, v_{0,n}, \theta_{0,l}\} \in \mathbb{R}^m$  is one feasible solution of the o-ACOPF model (1). From (1g) we have:

$$v_{0,sl}v_{0,rl} \sin \theta_{0,l} = X_l p_{0,sl} - R_l q_{0,sl}, \quad \forall l \in \mathcal{L} \quad (4a)$$

We can map  $\Omega_0$  to a feasible solution  $\Omega_1 = \{p_{1,n}, q_{1,n}, p_{1,sl}, q_{1,sl}, p_{1,ol}, q_{1,ol}, V_{1,n}, \theta_{1,l}\} \in \mathbb{R}^{m-n}$  of the SOC-ACOPF model (2) as:

$$\{\Omega_1 \setminus \theta_{1,l}\} := \{\Omega_0 \setminus (\theta_{0,l}, v_{0,n})\} \quad (4b)$$

$$\theta_{1,l} := v_{0,sl}v_{0,rl} \sin \theta_{0,l}, \quad \forall l \in \mathcal{L} \quad (4c)$$

Since  $v_{0,sl}v_{0,rl} \sin \theta_{0,l} \in (-1.21, 1.21) \subset (-\frac{\pi}{2}, \frac{\pi}{2})$ , equation (4c) is always mappable. Note  $\theta_{1,l}$  is not necessarily equal to  $\theta_{0,l}$ . On the other hand, mapping  $\Omega_1$  to  $\Omega_0$  ( $v_{0,sl}v_{0,rl} \sin \theta_{0,l} = \theta_{1,l}$ ) is not feasible when  $\theta_{1,l} > 1.21$  or  $\theta_{1,l} < -1.21$ .  $\square$

Theorem 1 shows that the feasible region of SOC-ACOPF model (2) covers all the feasible region of o-ACOPF model (1).

##### Theorem 2

If  $(\theta_l^{min}, \theta_l^{max}) \subseteq (-\frac{\pi}{2}, \frac{\pi}{2})$  and  $\theta_l^{min} = -\theta_l^{max}$ , the necessary condition of recovering (mapping) a feasible solution of the o-ACOPF model (1) from the (optimal) solution  $\Omega_1$  of SOC-ACOPF model (2) is:

$$V_{sl}V_{rl} \sin^2(\theta_l^{max}) \geq \theta_l^2, \quad \forall l \in \mathcal{L} \quad (4d)$$

Note constraint (4d) is conic and thus convex.

*Proof.* If a feasible solution  $\Omega_0$  of the o-ACOPF model (1) is recovered (mapped) from the (optimal) solution  $\Omega_1$  of the SOC-ACOPF model (2):

$$\{\Omega_0 \setminus (\theta_{0,l}, v_{1,n})\} := \{\Omega_1 \setminus (\theta_{1,l})\} \quad (4e)$$

$$v_{0,n} := \sqrt{V_{1,n}}, \quad \forall n \in N \quad (4f)$$

$$\begin{aligned}\theta_{0,l} &:= \arcsin\left(\frac{X_l p_{s1,l} - R_l q_{s1,l}}{v_{1,sl}v_{1,rl}}\right) \\ &= \arcsin\left(\frac{\theta_{1,l}}{v_{1,sl}v_{1,rl}}\right), \quad \forall l \in \mathcal{L}\end{aligned}\quad (4g)$$

Since  $\sin(\theta_{1,l})$  is monotonic in  $(\theta_l^{min}, \theta_l^{max}) \subseteq (-\frac{\pi}{2}, \frac{\pi}{2})$ , equation (4g) implies:

$$\sin(\theta_l^{min}) \leq \frac{\theta_{1,l}}{v_{s1,l}v_{r1,l}} \leq \sin(\theta_l^{max}), \quad \forall l \in \mathcal{L} \quad (4h)$$

Considering  $\sin^2(\theta_l^{min}) = \sin^2(\theta_l^{max})$  when  $\theta_l^{min} = -\theta_l^{max}$ , constraint (4h) is equivalent to:

$$\frac{\theta_{1,l}^2}{V_{s1,l}V_{r1,l} \sin^2(\theta_l^{max})} \leq 1, \quad \forall l \in \mathcal{L} \quad (4i)$$

Or  $V_{s1,l}V_{r1,l} \sin^2(\theta_l^{max}) \geq \theta_{1,l}^2$ .  $\square$

Theorem 2 shows that if we add the convex constraint (4d) to the SOC-ACOPF model (2), we can improve the solution feasibility towards the o-ACOPF model (1).

### Lemma 1

The SOC-ACOPF model (2) with the additional constraint (4d) is a relaxation of the o-ACOPF model (1).

*Proof.* We can use the same procedure in proving theorem 1 to prove lemma 1 i.e. any feasible solution of the o-ACOPF model (1) can be mapped to a feasible solution of the SOC-ACOPF model (2) with additional constraint (4d). However, the reverse statement is not true when there is at least one  $\hat{l} \in L$  (in the feasible solution of the SOC-ACOPF model (2) with the additional constraint (4d)) such that  $q_{o\hat{l}} > \frac{p_{s(r)\hat{l}}^2 + q_{s(r)\hat{l}}^2}{V_{s(r)\hat{l}}^*} X_{\hat{l}}$  (which fails to satisfy constraints (1e) in the ACOPF model (1) obviously).  $\square$

Lemma 1 shows that the SOC-ACOPF model (2) with the additional constraint (4d) still covers the feasible region of the o-ACOPF model (1).

### Lemma 2

If the optimal solution  $\Omega^*$  of the SOC-ACOPF model (2) with additional constraint (4d) gives tight relaxation  $q_{o\hat{l}}^* = \frac{p_{s(r)\hat{l}}^2 + q_{s(r)\hat{l}}^2}{V_{s(r)\hat{l}}^*} X_{\hat{l}}, \forall \hat{l} \in L$ , the global optimal solution  $\Omega_0^*$  of the ACOPF model (1) is  $\Omega_0^* := \{\Omega^* \setminus \theta_{\hat{l}}^*\} \cup \{v_{0,n}^* := \sqrt{V_n^*}, \theta_{0,l}^* := \arcsin(\frac{\theta_{\hat{l}}^*}{v_{s\hat{l}}^* v_{r\hat{l}}^*})\}$ .

*Proof.* Lemma 2 is a direct result of theorem 1, theorem 2 and lemma 1 considering the optimal objective solution  $f^*$  of the SOC-ACOPF model (2) is always a lower bound for the optimal objective solution  $f_0^*$  of the o-ACOPF model (1).  $\square$

### Theorem 3

Define the (parametric) optimal value functions:

$$f^*(p_{d_n}, q_{d_n}) := \min_{\Omega \in \mathbb{R}^m} f \text{ s.t. } \{\Omega \in \Omega_{ACOPF}\} \quad (4j)$$

$$f^*(p_{d_n}, q_{d_n}) := \min_{\Omega \in \mathbb{R}^{m-n}} f \text{ s.t. } \{\Omega \in \Omega_{SOC-ACOPF}\} \quad (4k)$$

Where  $\Omega_{ACOPF}$  and  $\Omega_{SOC-ACOPF}$  are the feasible regions of the o-ACOPF model (1) and SOC-ACOPF model (2) correspondingly. If the objective function  $f$  is a monotonically increasing function of  $(p_n, q_n)$  i.e.  $f(p_{1,n}, q_{1,n}) \leq f(p_{2,n}, q_{2,n})$  for  $(p_{1,n}, q_{1,n}) \leq (p_{2,n}, q_{2,n})$ , the optimal value functions  $f^*$  are monotonic i.e.  $f^*(p_{d_{1,n}}, q_{d_{1,n}}) \leq f^*(p_{d_{2,n}}, q_{d_{2,n}})$  if  $(p_{d_{1,n}}, q_{d_{1,n}}) \leq (p_{d_{2,n}}, q_{d_{2,n}})$  (assuming the o-ACOPF and SOC-ACOPF models are feasible for  $(p_{d_{1,n}}, q_{d_{1,n}})$  and  $(p_{d_{2,n}}, q_{d_{2,n}})$ ).

*Proof.* We prove theorem 3 by contradiction. Suppose the optimal solutions and objectives of the SOC-ACOPF (or o-ACOPF) model at  $(p_{d_{1,n}}, q_{d_{1,n}})$  and  $(p_{d_{2,n}}, q_{d_{2,n}})$  are  $\Omega_1^* = \{p_{1,n}^*, q_{1,n}^*, p_{1,s\hat{l}}^*, q_{1,s\hat{l}}^*, p_{1,o\hat{l}}^*, q_{1,o\hat{l}}^*, V_{1,n}^*, \theta_{1,l}^*\} \in \mathbb{R}^{m-n}$ ,  $f_1^*$  and  $\Omega_2^* = \{p_{2,n}^*, q_{2,n}^*, p_{2,s\hat{l}}^*, q_{2,s\hat{l}}^*, p_{2,o\hat{l}}^*, q_{2,o\hat{l}}^*, V_{2,n}^*, \theta_{2,l}^*\} \in \mathbb{R}^{m-n}$ ,  $f_2^*$ . If  $f_1^* > f_2^*$  for  $(p_{d_{1,n}}, q_{d_{1,n}}) \leq (p_{d_{2,n}}, q_{d_{2,n}})$ , since  $f$  is monotonic, there must be at least one  $\hat{n} \in N$  such that  $(p_{1,\hat{n}}^*, q_{1,\hat{n}}^*) > (p_{2,\hat{n}}^*, q_{2,\hat{n}}^*)$ . We can construct a feasible solution  $\Omega_1'$  of the SOC-ACOPF (or o-ACOPF) model at  $(p_{d_{1,n}}, q_{d_{1,n}})$  (by using  $\Omega_2^*$ ) as:

$$\{\Omega_1' \setminus (p_{1,\hat{n}}', q_{1,\hat{n}}')\} := \{\Omega_2^* \setminus (p_{2,\hat{n}}^*, q_{2,\hat{n}}^*)\} \quad (4l)$$

From (1b)-(1c), we have:

$$p_{2,\hat{n}}^* - p_{d_{2,\hat{n}}} = \sum_l (A_{\hat{n}l}^+ p_{s_{2,l}}^* - A_{\hat{n}l}^- p_{o_{2,l}}^*) + G_{\hat{n}} V_{2,\hat{n}}^* \quad (4m)$$

$$q_{2,\hat{n}}^* - q_{d_{2,\hat{n}}} = \sum_l (A_{\hat{n}l}^+ q_{s_{2,l}}^* - A_{\hat{n}l}^- q_{o_{2,l}}^*) - B_{\hat{n}} V_{2,\hat{n}}^* \quad (4n)$$

We know the feasible solution of  $(p_{1,\hat{n}}, q_{1,\hat{n}})$  must satisfy:

$$p_{1,\hat{n}}' - p_{d_{1,\hat{n}}} = \sum_l (A_{\hat{n}l}^+ p_{s_{2,l}}^* - A_{\hat{n}l}^- p_{o_{2,l}}^*) + G_{\hat{n}} V_{2,\hat{n}}^* \quad (4o)$$

$$q_{1,\hat{n}}' - q_{d_{1,\hat{n}}} = \sum_l (A_{\hat{n}l}^+ q_{s_{2,l}}^* - A_{\hat{n}l}^- q_{o_{2,l}}^*) - B_{\hat{n}} V_{2,\hat{n}}^* \quad (4p)$$

Substituting (4o)-(4p) to (4m)-(4n), we have:

$$p_{1,\hat{n}}' - p_{d_{1,\hat{n}}} = p_{2,\hat{n}}^* - p_{d_{2,\hat{n}}} \quad (4q)$$

$$q_{1,\hat{n}}' - q_{d_{1,\hat{n}}} = q_{2,\hat{n}}^* - q_{d_{2,\hat{n}}} \quad (4r)$$

Which yield:

$$p_{1,\hat{n}}' = p_{2,\hat{n}}^* + p_{d_{1,\hat{n}}} - p_{d_{2,\hat{n}}} \quad (4s)$$

$$q_{1,\hat{n}}' = q_{2,\hat{n}}^* + q_{d_{1,\hat{n}}} - q_{d_{2,\hat{n}}} \quad (4t)$$

So  $\Omega_1' = \{\Omega_2^* \setminus (p_{2,\hat{n}}^*, q_{2,\hat{n}}^*)\} \cup (p_{1,\hat{n}}', q_{1,\hat{n}}')$  is feasible for the SOC-ACOPF (or o-ACOPF) model. Because  $(p_{d_{1,n}}, q_{d_{1,n}}) \leq (p_{d_{2,n}}, q_{d_{2,n}})$ , equations (4s)-(4t) imply  $(p_{1,\hat{n}}', q_{1,\hat{n}}') \leq (p_{2,\hat{n}}^*, q_{2,\hat{n}}^*)$ . This means the corresponding objective function value  $f_1' \leq f_2^* < f_1^*$  (note  $(p_{1,\hat{n}}', q_{1,\hat{n}}') = (p_{2,\hat{n}}^*, q_{2,\hat{n}}^*) \forall \hat{n} \neq \hat{n}$ ) which contradicts the assumption that  $f_1^*$  is the optimal objective solution. So  $f_1^* > f_2^*$  cannot hold for  $(p_{d_{1,n}}, q_{d_{1,n}}) \leq (p_{d_{2,n}}, q_{d_{2,n}})$ . This completes the proof.  $\square$

### Theorem 4

Assuming  $(\theta_{\hat{l}}^{min}, \theta_{\hat{l}}^{max}) \subseteq (-\frac{\pi}{2}, \frac{\pi}{2})$  and the objective function  $f$  is monotonically increasing for  $(p_n, q_n)$ , if the optimal solution  $\Omega^*$  of the SOC-ACOPF model (2) (with additional constraint (4d)) at  $(p_{d_n}, q_{d_n})$  has positive relaxation gap  $q_{o\hat{l}}^* > \frac{p_{s(r)\hat{l}}^2 + q_{s(r)\hat{l}}^2}{V_{s(r)\hat{l}}^*} X_{\hat{l}}$  or  $p_{o\hat{l}}^* > \frac{p_{s(r)\hat{l}}^2 + q_{s(r)\hat{l}}^2}{V_{s(r)\hat{l}}^*} R_{\hat{l}}$  for some  $\hat{l} \in \mathcal{L}$ , there exists  $(p_{d_n}, q_{d_n}') > (p_{d_n}, q_{d_n})$  at which the relaxation is tight for the optimal solution i.e.  $q_{o\hat{l}}^* = \frac{p_{s(r)\hat{l}}^2 + q_{s(r)\hat{l}}^2}{V_{s(r)\hat{l}}^*} X_{\hat{l}} \forall \hat{l} \in \mathcal{L}$  or  $p_{o\hat{l}}^* = \frac{p_{s(r)\hat{l}}^2 + q_{s(r)\hat{l}}^2}{V_{s(r)\hat{l}}^*} R_{\hat{l}}$ .

*Proof.* To prove theorem 4, we firstly derive an equivalent model of the o-ACOPF model (1) by replacing constraint (1f) with:

$$V_{s\hat{l}} - v_{s\hat{l}} v_{r\hat{l}} \cos \theta_{\hat{l}} = p_{s\hat{l}} R_{\hat{l}} + q_{s\hat{l}} X_{\hat{l}}, \forall \hat{l} \in \mathcal{L} \quad (4u)$$

Constraints (4u)-and-(1g) are equivalent with constraints (1f)-and-(1g) for  $(\theta_{\hat{l}}^{min}, \theta_{\hat{l}}^{max}) \subseteq (-\frac{\pi}{2}, \frac{\pi}{2})$  since they are expressing the same voltage drop phasor either in the way of real-and-imaginary parts or amplitude-and-imaginary parts illustrated in Fig. 2.

We then define a new relaxed ACOPF model as r-ACOPF in (4v)

$$\text{Minimize}_{\Omega} \quad f(p_n, q_n, p_{o\hat{l}}, q_{o\hat{l}}) \quad (4v)$$

$$\text{subject to} \quad (1b) - (1c), (1j) - (1m)$$

$$(2b) - (2c), (4u) - (4a)$$

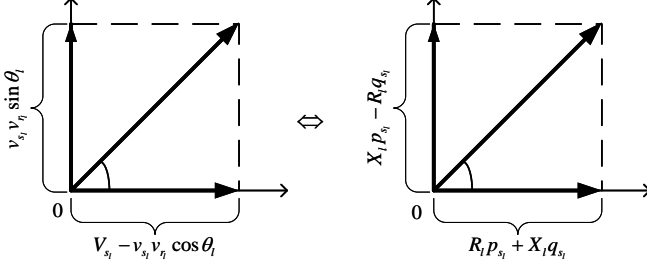


Fig. 2. Equivalent Constraint of the Voltage Drop Phasor

It is easy to show that, when the relaxation is tight, the feasible region of the r-ACOPF model (4v) is actually equivalent to the feasible region of the SOC-ACOPF model (2) (with additional constraint (4d)) since any feasible solution from either model (r-ACOPF or SOC-ACOPF) can be mapped to the feasible region of another model (SOC-ACOPF or r-ACOPF) using the procedures we derived in theorems 1-2. The feasible region comparison is shown in Fig. 3.

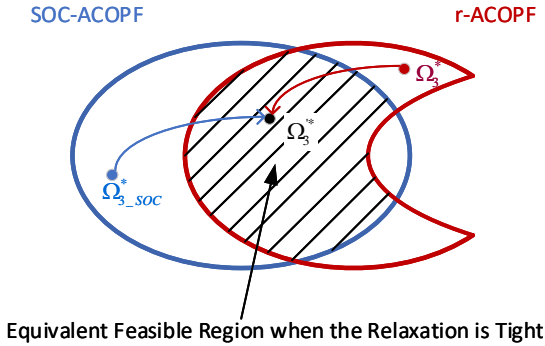


Fig. 3. Comparison of the Feasible Regions of SOC-ACOPF and r-ACOPF

We want to emphasize here that, although the r-ACOPF model (4v) is nonconvex (with regarding to its own set of variables), it is valid that part of its feasible region can be mapped to a convex one (with another set of variables) such as the convex SOC-ACOPF model (2) (with additional constraint (4d)). A obvious simple example is the the equivalence between the nonconvex region expressed by  $\{y = x^2, x > 0\}$  for  $(y, x) \in \mathbb{R}$  and convex region expressed by  $\{y = z, z > 0\}$  for  $(y, z) \in \mathbb{R}$ . Fig. 4 shows this equivalence graphically. A similar consideration can be drawn for the r-ACOPF model (4v) (where both  $V_n = v_n^2$  and  $v_n$  are deployed) and the SOC-ACOPF model (2) where only  $V_n$  are used.

Similarly, we define the (parametric) optimal value function of the r-ACOPF model (4v) (with regarding to  $(p_{d_n}, q_{d_n})$ ) as:

$$f^*(p_{d_n}, q_{d_n}) := \min_{\Omega \in \mathbb{R}^m} f \text{ s.t. } \{\Omega \in \Omega_{r-ACOPF}\} \quad (4w)$$

Following the same procedure in the proof of theorem 3, it is obvious that  $f^*$  here is also monotonic.

We now use the r-ACOPF model (4v) as a bridge to prove theorem 4. The key procedure is to show that 4 is valid for

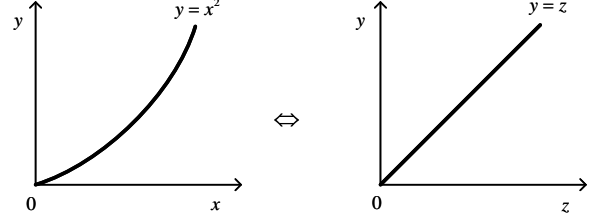


Fig. 4. The Equivalence of Regions Expressed by Different Variables

the r-ACOPF model (4v) and thus valid for the SOC-ACOPF model (2) considering the equivalence between their feasible regions (when the relaxation is tight). Suppose the optimal solution  $\Omega_3^*$  of the r-ACOPF model (4v) has positive relaxation gap  $q_{o3,i}^* > \frac{p_{3,s(r)\hat{l}}^{*2} + q_{3,s(r)\hat{l}}^{*2}}{V_{3,s(r)\hat{l}}^*} X_{\hat{l}}$  or  $p_{o3,i}^* > \frac{p_{3,s(r)\hat{l}}^{*2} + q_{3,s(r)\hat{l}}^{*2}}{V_{3,s(r)\hat{l}}^*} R_{\hat{l}}$  for some  $\hat{l} \in \mathcal{L}$  at  $(p_{d_n}, q_{d_n})$ , we use  $\Delta^* p_{o3,i} > 0$  and  $\Delta^* q_{o3,i} > 0$  to represent the active and reactive power losses relaxation gap respectively:

$$p_{o3,i}^* - \frac{p_{3,s(r)\hat{l}}^{*2} + q_{3,s(r)\hat{l}}^{*2}}{V_{3,s(r)\hat{l}}^*} R_{\hat{l}} = \Delta^* p_{o3,i} \quad (4x)$$

$$q_{o3,i}^* - \frac{p_{3,s(r)\hat{l}}^{*2} + q_{3,s(r)\hat{l}}^{*2}}{V_{3,s(r)\hat{l}}^*} X_{\hat{l}} = \Delta^* q_{o3,i} \quad (4y)$$

So the tight power losses solutions are  $p_{o3,i}' = p_{o3,i}^* - \Delta^* p_{o3,i} > 0$  and  $q_{o3,i}' = q_{o3,i}^* - \Delta^* q_{o3,i} > 0$ . From constraints (1b)-(1c), we have:

$$p_{3,n}^* - p_{d_n} = \sum_l (A_{nl}^+ p_{s3,l}^* - A_{nl}^- p_{o3,l}^*) + G_n V_{3,n}^* \quad (4z)$$

$$q_{3,n}^* - q_{d_n} = \sum_l (A_{nl}^+ q_{s3,l}^* - A_{nl}^- q_{o3,l}^*) - B_n V_{3,n}^* \quad (4aa)$$

Suppose at  $(p_{d_n}', q_{d_n}')$ , tight power losses solutions are found (note in the r-ACOPF model only following constraints are associated with the power losses variables aside from constraints (2b)-(2c)):

$$p_{3,n}' - p_{d_n}' = \sum_l (A_{nl}^+ p_{s3,l}' - A_{nl}^- p_{o3,l}') + G_n V_{3,n}' \quad (4ab)$$

$$q_{3,n}' - q_{d_n}' = \sum_l (A_{nl}^+ q_{s3,l}' - A_{nl}^- q_{o3,l}') - B_n V_{3,n}' \quad (4ac)$$

Combining equations (4z)-(4aa) with equations (4ab)-(4ac), we have:

$$p_{d_n}' = p_{d_n} - \sum_l A_{nl}^- \Delta^* p_{o3,l}^* \quad (4ad)$$

$$q_{d_n}' = q_{d_n} - \sum_l A_{nl}^- \Delta^* q_{o3,l}^* \quad (4ae)$$

Because  $A_{nl}^- \in \{0, -1\}$  and  $(\Delta^* p_{o3,l}^*, \Delta^* q_{o3,l}^*) > 0$ , equations (4ad)-(4ae) imply  $(p_{d_n}', q_{d_n}') > (p_{d_n}, q_{d_n})$ . Taking into account that the optimal value function  $f^*$  is monotonic, we also know that  $f^*(p_{d_n}, q_{d_n}) < f^*(p_{d_n}', q_{d_n}')$  which means  $(p_{d_n}', q_{d_n}')$  is not only feasible but also optimal for the r-ACOPF model (4v).

As we have explained at the beginning of this proof, since the r-ACOPF model (4v) is actually equivalent (in terms of the feasible region and optimal solution when the relaxation is tight) with the SOC-ACOPF model (2), all the tight solutions we derived in proving theorem 4 for the r-ACOPF model (4v) can always be mapped to the corresponding tight solution of the SOC-ACOPF model (2). In other words, theorem 4 is also valid for the SOC-ACOPF model (2).  $\square$

Theorem 4 shows the structure of the relaxed solutions and tight solutions for the SOC-ACOPF model (2) with regarding to the load absorption parameter. This theorem shows a counter-intuitive property of the SOC-ACOPF model (2) that larger power load can help tighten the relaxation gap. We present in the next section the numerical validations of all the theorems and analysis in this section.

## V. NUMERICAL RESULTS AND DISCUSSION

The SOC-ACOPF model (2) and o-ACOPF model (1) are implemented in the YALMIP [22] toolbox for modelling and optimization in MATLAB running on the 64-bit macOS operating system. A personal computer with Intel Core i9 2.9 GHz CPU and 16G RAM is deployed. The MOSEK or SCS solver is used to solve the SOC-ACOPF model (2). Because MOSEK and SCS can only solve convex models, the convexity of the SOC-ACOPF model (2) is numerically validated. The IPOPT solver is used to solve the nonconvex o-ACOPF model (1). We use IEEE test cases (14, 57, 118, 300), 1354pegase and 2869pegase [23] to validate our proposed theorems in this Section. Power network data from MATPOWER are directly used here [24]. The objective function  $f$  of typical economic dispatch is quadratic i.e.  $f(p_n) = \sum_n \alpha_n p_n^2 + \beta_n p_n$ . Where  $(\alpha_n, \beta_n) \geq 0$  are the cost parameters of the nodal active power injections. Note that to make sure the objective function  $f$  is monotonic for  $p_n$ , we must ensure  $p_n^{min} \geq 0$  in the o-ACOPF and SOC-ACOPF models.

Since we have tested our models for the base load and shown in our previous work [25] that large relaxation gaps are present for optimal solutions in low load levels, we only show the results for low load levels here. In Table I, we list the objective solutions of the SOC-ACOPF model (2) and the o-ACOPF model (1) for 10%, 20%, 30%, 40% and 50% of the absolute value of base load. So, the results in Table I validate two of our theorems: (i) SOC-ACOPF model (2) is a relaxation of the o-ACOPF model (1). This is validated since all the objective solutions of the SOC-ACOPF model (2) is lower than the o-ACOPF model (1); (ii) the optimal value functions of the SOC-ACOPF model (2) and the o-ACOPF model (1) are monotonic (with regarding to power load  $p_d$ ) given that the objective function  $f$  is monotonic with regarding to  $p_n$ . This is validated since all the objective solutions increase when the power load levels increase.

For the SOC-ACOPF model (2), the relaxation gaps of active power losses and reactive power losses are defined as (5a)-

(5b):

$$Gap_l^{po} = p_{o_l} - \frac{p_{s_l}^2 + q_{s_l}^2}{V_{s_l}} R_l \quad (5a)$$

$$Gap_l^{qo} = q_{o_l} - \frac{p_{s_l}^2 + q_{s_l}^2}{V_{s_l}} X_l \quad (5b)$$

The maximum relaxation gaps (of active and reactive power losses) are defined as  $Gap^{po,max} = \text{Maximum}\{Gap_l^{po}, \forall l \in \mathcal{L}\}$  and  $Gap^{qo,max} = \text{Maximum}\{Gap_l^{qo}, \forall l \in \mathcal{L}\}$ . We use  $Gap^{po,max}$  and  $Gap^{qo,max}$  to measure the the relaxation performance of the SOC-ACOPF model (2) (smaller relaxation gaps mean better performance). We list the maximum relaxation gaps results  $Gap^{po,max}$  and  $Gap^{qo,max}$  of the SOC-ACOPF model (2) in Table II and Table III. When the relaxation is not tight, we increase the power load levels ( $p_d, q_d$ ) (but fix the optimal nodal power injection solution  $p_n^*$  so the objective solutions remain the same as in Table I) to find the tight solutions of the SOC-ACOPF model (2). The maximum relaxation gaps for tight solutions are listed in the columns denoted as '>10% Load', '> 20% Load', '> 30% Load', '> 40% Load' and '> 50% Load' of Table II and Table III. So we have actually numerically validated theorem 4 by the results in Table II and Table III. It is worth to mention that for most branches, the relaxation gaps are very small. The maximum relaxation gap only appear for single branch in each test case.

## VI. CONCLUSIONS

By equivalently deriving the ampacity constraint of branch for the power losses variable, we firstly fill the approximation gap of the SOC-ACOPF model (2) based on the branch flow formulation. We then give the analytical and numerical proofs for several important properties of the SOC-ACOPF model (2). The aims of proving these properties are to improve the solution quality and to promote the applicability of the SOC-ACOPF model (2). We show rigorously that the feasible region of the SOC-ACOPF model (2) covers the feasible region of the o-ACOPF model (1). Regarding to the AC feasibility of the solution from the SOC-ACOPF model (2), one additional necessary conic constraint to improve the AC feasibility of the solution is derived in theorem 2. We also show how to recover the global optimal solution of the o-ACOPF model (1) from the tight optimal solution of the SOC-ACOPF model (2) in theorem 2. Based on the monotonic property of the optimal value functions defined by the SOC-ACOPF model (2) and the o-ACOPF model (1) from theorem 3, we prove that the tight solutions of the SOC-ACOPF model (2) can always be obtained by allowing the increase of nodal load absorptions in theorem 4. This structure shows that large power load levels actually help tighten the relaxation gap of the SOC-ACOPF model (2). Future work to investigate more properties or applications of the SOC-ACOPF model (2) are expected.

## REFERENCES

- [1] J. Carpentier, "Contribution to the economic dispatch problem," *Bulletin of the French Society of Electricians*, vol. 3, no. 8, pp. 431-447, 1962.
- [2] M. B. Cain, R. P. Oneill, and A. Castillo, "History of optimal power flow and formulations," FERC, Tech. Rep., 2012.

TABLE I  
OBJECTIVE SOLUTIONS

Test case	10% Load		20% Load		30% Load		40% Load		50% Load	
	SOC-ACOPF	o-ACOPF	SOC-ACOPF	o-ACOPF	SOC-ACOPF	o-ACOPF	SOC-ACOPF	o-ACOPF	SOC-ACOPF	o-ACOPF
IEEE14	545.64	546.37	1147.21	1147.50	1806.10	1806.26	2523.77	2523.91	3301.57	3301.75
IEEE57	2682.55	2686.41	5706.04	5709.00	9080.48	9082.93	12809.00	12810.65	16894.49	16896.07
IEEE118	8940.49	8952.62	18735.71	18750.11	29420.72	29436.19	41008.27	41025.36	53515.24	53533.33
IEEE300	51210.16	56915.23	107284.01	108378.18	168588.72	168712.09	235157.51	235244.97	307031.10	307102.32
1354pegase	7558.35	7558.47	15101.85	15102.06	22665.28	22665.88	30246.88	30249.40	37849.92	37853.77
2869pegase	14639.05	14754.46	29204.10	29236.82	43811.78	43830.34	58458.84	58467.05	73133.48	73142.93

TABLE II  
MAXIMUM RELAXATION GAPS OF ACTIVE POWER LOSSES FROM THE SOC-ACOPF MODEL

Test case	10% Load	>10% Load	20% Load	>20% Load	30% Load	>30% Load	40% Load	>40% Load	50% Load	>50% Load
IEEE14	5.43E-10	7.31E-13	3.35E-09	6.89E-13	1.06E-10	6.85E-12	2.99E-09	1.45E-12	4.31E-09	4.30E-12
IEEE57	1.84E-10	5.92E-10	2.52E-11	7.46E-10	1.36E-09	2.09E-10	6.38E-09	8.26E-10	3.99E-10	3.56E-10
IEEE118	4.93E-09	3.28E-09	6.02E-08	1.79E-09	1.11E-07	1.10E-09	1.57E-09	3.99E-11	1.09E-07	4.34E-10
IEEE300	1.15E-02	4.14E-08	1.37E-03	8.17E-09	4.08E-06	2.52E-09	5.01E-05	1.10E-09	2.88E-05	7.83E-10
1354pegase	3.09E-03	1.79E-07	2.72E-07	1.42E-07	1.01E-02	1.43E-07	1.04E-02	1.03E-07	9.79E-03	5.30E-08
2869pegase	8.47E-03	7.12E-06	9.32E-03	1.38E-07	6.72E-03	6.56E-08	1.47E-02	6.99E-08	1.41E-02	8.22E-08

TABLE III  
MAXIMUM RELAXATION GAPS OF REACTIVE POWER LOSSES FROM THE SOC-ACOPF MODEL

Test case	10% Load	>10% Load	20% Load	>20% Load	30% Load	>30% Load	40% Load	>40% Load	50% Load	>50% Load
IEEE14	2.50E-01	8.51E-11	7.95E-02	3.92E-11	1.43E-01	1.24E-10	1.18E-01	2.33E-11	9.32E-02	1.36E-11
IEEE57	2.25E-01	2.00E-09	1.92E-01	9.65E-09	1.46E-01	3.10E-09	1.02E-01	3.37E-09	1.28E-01	1.39E-09
IEEE118	2.98E+00	1.00E-08	3.08E+00	1.37E-08	2.86E+00	9.55E-09	2.84E+00	3.03E-09	3.04E+00	1.35E-08
IEEE300	5.25E+00	9.33E-08	4.12E+00	1.75E-08	3.82E+00	3.26E-08	3.62E+00	6.55E-08	2.97E+00	6.50E-08
1354pegase	2.95E-01	1.46E-06	2.93E-01	3.45E-07	8.50E-01	4.77E-07	8.74E-01	2.63E-07	8.21E-01	2.63E-07
2869pegase	7.81E-01	4.96E-05	5.03E-01	3.44E-06	3.79E-01	8.79E-07	2.64E+00	1.12E-06	2.52E+00	6.11E-07

- [3] P. Panciatici, M. C. Campi, S. Garatti, S. H. Low, D. K. Molzahn, A. X. Sun, and L. Wehenkel, "Advanced optimization methods for power systems," in *2014 Power Systems Computation Conference*, Aug 2014, pp. 1–18.
- [4] M. Farivar and S. H. Low, "Branch Flow Model: Relaxations and Convexification: Part I, Part II," *IEEE Transactions on Power Systems*, vol. 28, no. 3, pp. 2554–2572, Aug 2013.
- [5] L. Gan, N. Li, U. Topcu, and S. H. Low, "Exact convex relaxation of optimal power flow in radial networks," *Automatic Control, IEEE Transactions on*, vol. 60, no. 1, pp. 72–87, 2015.
- [6] B. Kocuk, S. S. Dey, and X. A. Sun, "Strong socp relaxations for the optimal power flow problem," *Operations Research*, vol. 64, pp. 1177–1196, 2016.
- [7] X. Bai, H. Wei, K. Fujisawa, and Y. Wang, "Semidefinite programming for optimal power flow problems," *International Journal of Electrical Power & Energy Systems*, vol. 30, no. 6, pp. 383–392, 2008.
- [8] J. Lavaei and S. H. Low, "Zero duality gap in optimal power flow problem," *Power Systems, IEEE Transactions on*, vol. 27, no. 1, pp. 92–107, 2012.
- [9] D. K. Molzahn and I. A. Hiskens, "Moment-based relaxation of the optimal power flow problem," in *2014 Power Systems Computation Conference*, Aug 2014, pp. 1–7.
- [10] —, "Sparsity-exploiting moment-based relaxations of the optimal power flow problem," *IEEE Transactions on Power Systems*, vol. 30, no. 6, pp. 3168–3180, Nov 2015.
- [11] H. Hijazi, C. Coffrin, and P. V. Hentenryck, "Convex quadratic relaxations for mixed-integer nonlinear programs in power systems," *Mathematical Programming Computation*, vol. 9, no. 3, pp. 321–367, Sep 2017.
- [12] C. Coffrin, H. L. Hijazi, and P. V. Hentenryck, "The QC Relaxation: A Theoretical and Computational Study on Optimal Power Flow," *IEEE Transactions on Power Systems*, vol. 31, no. 4, pp. 3008–3018, July 2016.
- [13] C. Coffrin, H. L. Hijazi, and P. Van Hentenryck, "Strengthening convex relaxations with bound tightening for power network optimization," in *Principles and Practice of Constraint Programming*, G. Pesant, Ed. Cham: Springer International Publishing, 2015, pp. 39–57.
- [14] M. Bynum, A. Castillo, J. Watson, and C. D. Laird, "Tightening mccormick relaxations toward global solution of the acopf problem," *IEEE Transactions on Power Systems*, vol. 34, no. 1, pp. 814–817, Jan 2019.
- [15] M. E. Baran and F. F. Wu, "Optimal capacitor placement on radial distribution systems," *IEEE Transactions on Power Delivery*, vol. 4, no. 1, pp. 725–734, Jan 1989.
- [16] R. Jabr *et al.*, "Radial distribution load flow using conic programming," *Power Systems, IEEE Transactions on*, vol. 21, no. 3, pp. 1458–1459, 2006.
- [17] K. Christakou, D.-C. Tomozei, J.-Y. L. B. Boudec, and M. Paolone, "AC OPF in Radial Distribution Networks-Parts I, II," *Electric Power Systems Research*, vol. 143, 150, pp. 438 – 450, 24–35, 2017.
- [18] M. Nick, R. Cherkaoui, J. L. Boudec, and M. Paolone, "An exact convex formulation of the optimal power flow in radial distribution networks including transverse components," *IEEE Transactions on Automatic Control*, vol. 63, no. 3, pp. 682–697, March 2018.
- [19] D. Shchetinin, T. A. Tinoco De Rubira, and G. Hug-Glanzmann, "Efficient bound tightening techniques for convex relaxations of ac optimal power flow," *IEEE Transactions on Power Systems*, pp. 1–1, 2019.
- [20] D. Shchetinin, T. T. De Rubira, and G. Hug, "On the construction of linear approximations of line flow constraints for ac optimal power flow," *IEEE Transactions on Power Systems*, vol. 34, no. 2, pp. 1182–1192, March 2019.
- [21] Z. Yuan, M. R. Hesamzadeh, and D. Biggar, "Distribution locational marginal pricing by convexified ACOF and hierarchical dispatch," *IEEE Transactions on Smart Grid*, vol. PP, no. 99, pp. 1–1, 2016.
- [22] J. Löfberg, "Yalmip : A toolbox for modeling and optimization in matlab," in *In Proceedings of the CACSD Conference*, Taipei, Taiwan, 2004.
- [23] S. Fliscounakis, P. Panciatici, F. Capitanescu, and L. Wehenkel, "Contingency ranking with respect to overloads in very large power systems taking into account uncertainty, preventive, and corrective actions," *IEEE Transactions on Power Systems*, vol. 28, no. 4, pp. 4909–4917, Nov 2013.
- [24] R. D. Zimmerman, C. E. Murillo-Sánchez, and R. J. Thomas, "Matpower: Steady-state operations, planning, and analysis tools for power systems research and education," *Power Systems, IEEE Transactions on*, vol. 26, no. 1, pp. 12–19, 2011.
- [25] Z. Yuan and M. R. Hesamzadeh, "Second-order cone AC optimal power flow: convex relaxations and feasible solutions," *Journal of Modern Power Systems and Clean Energy*, vol. 7, no. 2, pp. 268–280, Mar 2019.